Progress In Electromagnetics Research B, Vol. 4, 27–39, 2008

MICROSTRIP ANTENNA WITH DEFECTED GROUND PLANE STRUCTURE AS A SENSOR FOR LANDMINES DETECTION

S. H. Zainud-Deen, M. E. Badr, E. El-Deen, K. H. Awadalla and H. A. Sharshar

Faculty of Electronic Engineering
Menoufia University
Menouf, Egypt

Abstract—A proposed sensor for landmines detection consists of two parallel microstrip antennas placed on the same ground plane and with defected ground structure between them has been investigated. The microstrip patch array with defected ground structure has the advantage of a low mutual coupling compared with the classic one. The Finite-Difference Time-Domain (FDTD) is used to simulate the sensor for landmines detection.

1. INTRODUCTION

Landmines are explosive devices placed on or beneath the surface of the earth for the purpose of destroying vehicles and killing or maiming human beings. Mines are usually deployed during a military conflict; however, they may remain in the ground undetected for decades after the cessation of hostilities. The United Nations estimates that there are currently over 199 million land mines buried in 71 countries throughout the world, and that the number of deployed mines increases by approximately 2 million each year. Accidental detonation of mines kills or maims 2000 or more people a month, predominantly civilians. The resulting injuries have devastating effects on the lives of the wounded and place incredible demands on the health, welfare, and social systems of the nations involved. There is presently no reliable means for detecting these hidden mines. Landmines have many social and economical impacts which can not be described by simple quantitative measures. Many communities have not been involved in proper clearance activities and have adapted to situation in their own ways. Global Landmine Survey is an international effort to

understand the socio-economic impact of landmines and unexploded ordnance (UXO). Without knowing the impacts, it is difficult to develop strategies to allocate limited resources to minimize the effect of landmines. Landmine resources compete with other humanitarian activities. The low and decreasing mortality from landmines is often compared to high and soaring mortality from epidemic disease. It is becoming clear that complete clearance is not a feasible solution of the worldwide landmine problem when the size of contaminated area is considered into account. That is why it is essential to understand the social and economical impacts of landmines [1–5].

Recent straggle in foreign lands have highlighted the need for effective mine location sensors. Thus, an important requirement for an electromagnetic sensor operating at a radio or microwave frequency is the ability to detect nonmetallic and metallic mines. A separated-aperture sensor has been investigated in [6]. Using the mutual coupling behavior between the transmitting and receiving dipoles the presence of a buried target is determined. Recently two patch array antennas have been proposed for the detection of buried land mines [7–9].

Microstrip (patch) antennas are known to strongly radiate in directions along the ground plane. A problem is encountered in arrays of patches that are printed on the same substrate: strong coupling among the arrays element. This coupling can be attributed to the surface-wave coupling. Which are guided by the substrate and the ground plane. Some different efficient techniques are explicitly designed to suppress the surface-waves, to reduce the mutual coupling between the antenna elements. They include optimizing grooving the dielectric, covering the patch by additional dielectric layer, placing shorting posts (pins) between the patch and the ground, or making the dielectric be a band gap structure by printing various pattern on it, or machining the dielectric below the patch, so that there is air below the patch, removing the dielectric between the two patch element [10]

Recently *a defected ground structure* (DGS) have been introduced, DGS is realized by etching off a simple shape defected from the ground plane, depending on the shape and dimensions of the defect, the shielded current distribution in the ground plane is disturbed resulting a controlled excitation and propagation of the electromagnetic waves through the substrate layer. Defected ground structures, either in a single configuration or periodic form that is frequently referred to as a photonic band gap (PBG) show slow-wave effects leading to considerable size realization. A geometry of a dumb-bell shaped DGS etched on the ground plane between the two patch arrays elements. The dimension of the DGS is optimized for the band gap at the resonant frequency of the antenna by trial and error approach. The

square lattice dimension is $(a \times b)$, with etch gap distance g and width of the gap w [11].

In this paper, a proposed sensor for landmines detection consists of two parallel microstrip antennas placed on the same ground plane with defected ground structure between the arrays has been investigated. A finite-difference time-domain (FDTD) program developed by the authors is used in the analysis. The numerical results are given in Section 2, and the conclusions are given in Section 3.

2. NUMERICAL RESULTS

Due to high excitation of surface waves in the E-plane coupled microstrip patches. It was simulated to investigate the effect of DGS on the element's mutual coupling. The mutual coupling $|S_{21}|$ between two coaxial fed microstrip antennas elements with infinite smooth ground plane and microstrip antenna with defected ground structure have been calculated using the FDTD [12, 13]. The dimensions of the patch after scaling it from 6 GHz [11] to 790 MHz: are, the patch length $L = 53.16308\,\text{mm}$, patch width $W = 45.568\,\text{mm}$, substrate thickness $h = 9.645\,\text{mm}$, the feed position at $y = 20.5056\,\text{mm}$, and $x = 22.784\,\text{mm}$, the dielectric substrate material $\varepsilon_r = 10.2$ at resonant frequency $f_o = 790\,\text{MHz}$. Fig. 1(a) show top and bottom view of classical two elements with infinite smooth ground plane E-plane arrays element. The defected ground structure dimension in the ground plane dimensions are: the width of defected $a = 27.341\,\text{mm}$, the length of the defected $b = 30.3789\,\text{mm}$, the gap length between the two square defected $g = 6.835\,\text{mm}$, and the gap width $w = 9.1136\,\text{mm}$. Fig. 1(b) and Fig. 1(c) show top and bottom view of the defected ground structure E-plane arrays elements.

The E-plane mutual coupling has been calculated versus the spacing (S/λ_o), for both the classical patch arrays and the classical with defective ground structure. The space steps used for FDTD are $\Delta x = 2.2784\,\text{mm}$, $\Delta y = 2.2784\,\text{mm}$, and $\Delta z = 1.929\,\text{mm}$, and the number of iterations is 15,000 time step. As shown the classical antenna shows a very strong coupling of $-15\,\text{dB}$ for the spacing between the elements $\lambda_o/2 = 189.873\,\text{mm}$. This is due to high surface wave in thick and high permittivity substrate. While the mutual coupling for the antenna with defected ground plane is $-24.0\,\text{dB}$, since the resonant frequency of the antenna falls inside the DGS band gap. Thus the surface waves are suppressed and the simulation shows that the mutual coupling drops by 9 dB lower than the classical antenna as shown in Fig. 2. As the separation increases, the mutual coupling for the classical antenna decreases, but for antenna with

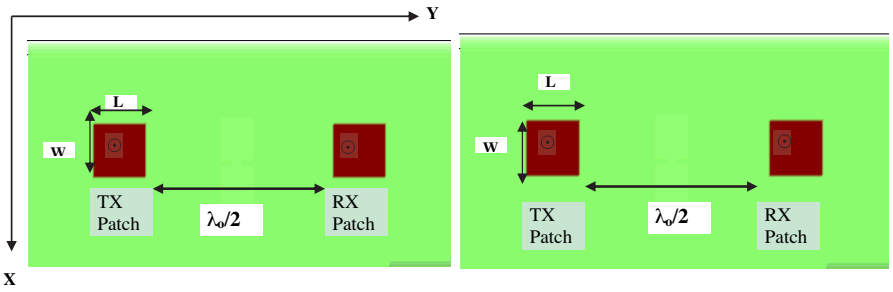

(a) Top view of Classical two patch arrays elements with smooth ground plane, with space = λ□/2 and substtrate with $\varepsilon_r = 10.2$.

(b) Top view of DGS two patch arrays elements with space λ□/2 on substrate with $\varepsilon_r = 10.2$.

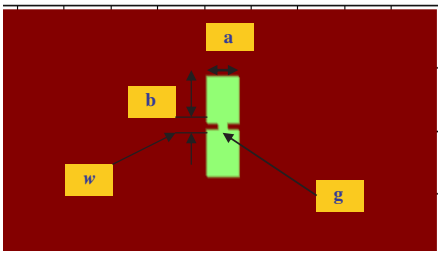

(c) Bottom view of Ground plane with defected ground structure with dimensions, a = 27.341 mm, b = 30.3789 mm, w = 9.1136 and g = 6.835.

Figure 1. Top and bottom view of two patch arrays antenna coaxial fed Geometry at $f_o = 790$ MHz. (a) Top view of classical arrays with smooth ground plane, (b) top view of DGS arrays, and (c) bottom view of defected ground plane of DGS arrays.

DGS contradictory phenomena occurs. As the separation increases the coupling increases, this is because the DGS band gap is no longer centered at the antenna resonant frequency which leads to higher coupling Based on the previous section, two types of sensors have been constructed at $f_o = 790$ MHz for landmines detection.

The first sensor consists of two microstrip patch arrays elements with smooth ground plane (classical sensor). The construction of the sensor and landmine is shown in Fig. 3(a). Each microstrip patch antenna consists of a rectangular patch with dimension as: the patch length $L = 53.16308$ mm, patch width $W = 45.568$ mm, substrate thickness $h = 9.645$ mm, the feed position at $y = 20.5056$ mm, and $x = 22.784$ mm, the dielectric substrate material $\varepsilon_r = 10.2$ at resonant

frequency $f_o = 790\,\text{MHz}$. The sensor with an infinite size ground plane is considered.

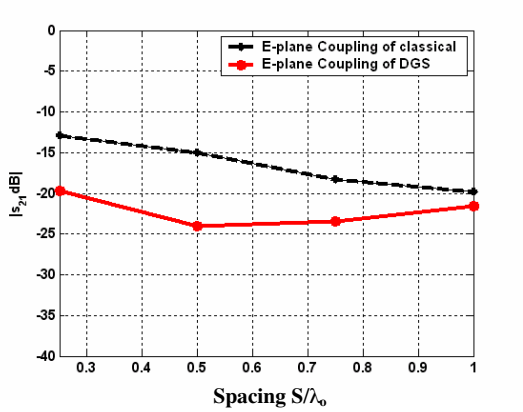

Figure 2. The calculated $|S_{21}|$, of the E-plane classic arrays and DGS arrays.

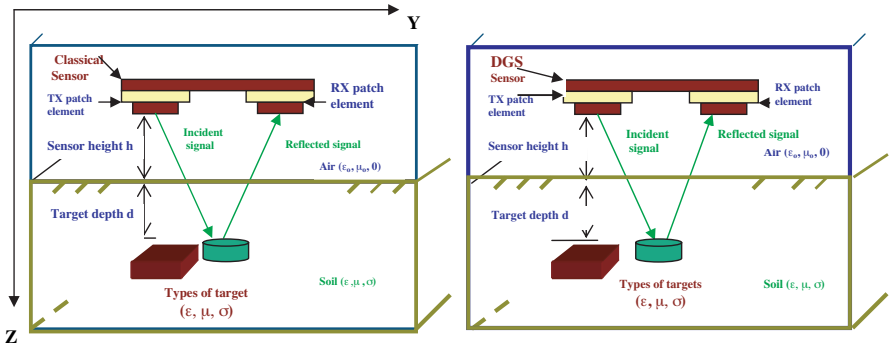

(a) Without defected ground structure (b) With defected ground plane structure

Figure 3. Geometry of the whole problem for landmines detection, the domain includes the sensor in air at certain height (h) from the surface of the ground, the soil properties, and the target properties buried at depth (d).

The second sensor consists of two microstrip patch with defected ground plane structure between them at frequency $f_o = 790\,\text{MHz}$ (DGS sensor), with the same dimensions of classical sensor, but the defected ground structure dimensions consists of two square lattice with length $a = 27.341\,\text{mm}$, $b = 30.3789\,\text{mm}$ and separated by

gap with length $w = 9.1136$ and width $g = 6.835$ as shown in Fig. 3(b).

FDTD simulation has been carried out to calculate the detection capability of the two sensors under investigations, the classical sensor and the DGS sensor. Different types of soil with two different types of targets (mines) have been detecting using both sensors. The sensor is located in air at height $h = 2.8\,\text{cm}$, from the surface of the ground, while the target is buried at depth of 7.5 cm under the ground inside the soil.

In the first case, the soil is described as "Fairly dry, loamy soil", with an electrical properties of $\varepsilon_r = 2.9$, $\mu_r = 1.0$, and $\sigma = 0.02\,\text{s/m}$. Different types of buried targets have been detected inside the soil. *The first buried target* is PMN-mine (with relatively circular mine with bakelite body), its electrical properties is $\varepsilon_r = 4.5$, $\mu_r = 1.0$, $\sigma = 0.07\,\text{s/m}$, weight = 550 g, its diameter = 110 mm, and height = 55 mm. a rubber membrane cover the top of the mine and is held in place by a thin metal band, the TNT material with electrical properties of $\varepsilon_r = 3.0$, $\mu = 1.0$, and $\sigma = 0.0029\,\text{s/m}$. Fig. 4 shows the calculated mutual coupling, $|S_{21}|$, resulting from using the classical sensor in case of the absence the presence of the target is $-20.78\,\text{dB}$ and $-25.04\,\text{dB}$, respectively. The difference between the two cases is about $-4.22.0\,\text{dB}$.

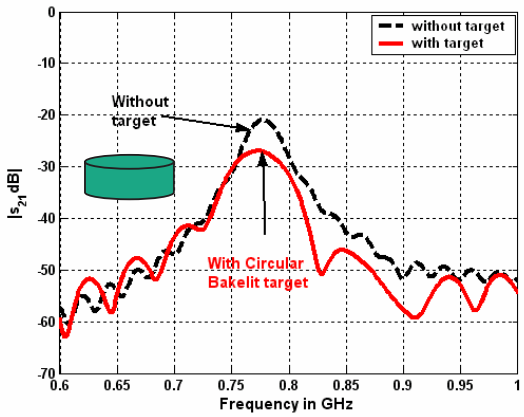

Figure 4. $|S_{21}|$ of classic sensor to detect circular Bakelite target buried in soil with $\varepsilon_r = 2.9$, using FDTD simulation at $f_o = 790\,\text{MHz}$.

If the DGS sensor is simulated to detect the same *bakelite target* with the same electrical properties in the same soil properties. Fig. 5 shows the calculated mutual coupling, $|S_{21}|$, resulting from using the DGS sensor in case of the absence and presence of the target is $-29.2\,\text{dB}$ and $-20.78\,\text{dB}$, respectively. The difference is about

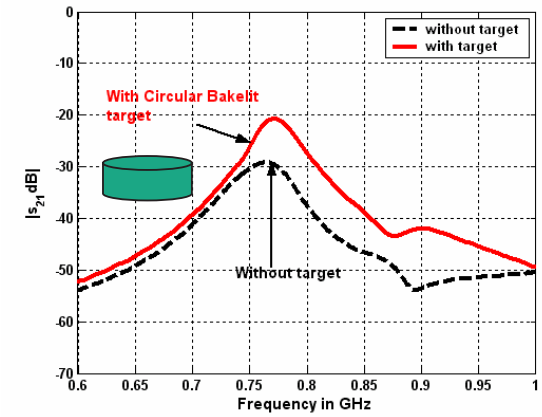

Figure 5. $|S_{21}|$ of DGS sensor to detect circular Bakelite target buried in soil with $\varepsilon_r = 2.9$ using FDTD simulation at $f_o = 790\,\text{MHz}$.

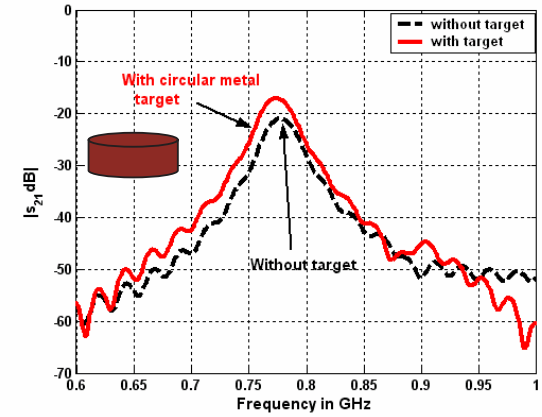

Figure 6. $|S_{21}|$ of classic sensor to detect circular metal target buried in soil with $\varepsilon_r = 2.9$ using FDTD simulation at $f_o = 790\,\text{MHz}$.

8.42 dB. The DGS sensor enhanced the detection of the buried target by $\sim 8.42\,\text{dB}$.

If the buried target in the same soil is *circular metal target* contains TNT material. The target characteristics are circular shape with diameter = 110 mm, height = 55 mm, weight = 550 g, and $\sigma = 58 \times 10^{12}\,\text{s/m}$, Fig. 6 shows the calculated mutual coupling, $|S_{21}|$, resulting from using the classical sensor in case of the absence the presence of the target is $-20.78\,\text{dB}$ and $-17\,\text{dB}$, respectively. The

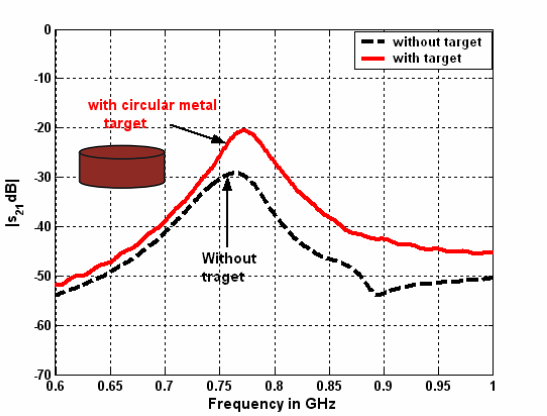

Figure 7. $|S_{21}|$ of DGS Sensor to detect circular metal target buried in soil with $\varepsilon_r = 2.9$ using FDTD simulation at $f_o = 790\,\text{MHz}$.

difference between the two cases is enhanced by $\sim 3.78\,\text{dB}$.

If the DGS sensor is simulated to detect the same *circular metal target* with same electrical properties in the same soil properties. Fig. 7 shows the calculated mutual coupling, $|S_{21}|$, resulting from using the DGS sensor in case of the absence and presence of the target is $-29.2\,\text{dB}$ and $-20.5\,\text{dB}$, respectively. The difference is about $8.75\,\text{dB}$. The DGS sensor enhanced the detection of the buried target by $\sim 8.7\,\text{dB}$.

If the buried target in the same soil is *metal block target* contains TNT material. The target characteristics are block shape with length $= 241.15\,\text{mm}$, width $= 86.57\,\text{mm}$, depth $= 55.94\,\text{mm}$, weight $= 100\,\text{g}$, and $\sigma = 58 \times 10^{12}\,\text{s/m}$. The TNT material with electrical properties of $\varepsilon_r = 3.0$, $\mu = 1.0$, and $\sigma = 0.0029\,\text{s/m}$. Fig. 8 shows the calculated mutual coupling, $|S_{21}|$, resulting from using the classical sensor in case of the absence the presence of the target is $-20.78\,\text{dB}$ and $-22.5\,\text{dB}$, respectively. The difference between the two cases is decreases by $2\,\text{dB}$.

If the DGS sensor is simulated to detect the above *metal block target* with same electrical properties and in the same soil properties. Fig. 9 shows the calculated mutual coupling, $|S_{21}|$, resulting from using the DGS sensor in case of the absence and presence of the target is $-29.2\,\text{dB}$ and $-19.5\,\text{dB}$, respectively. The difference is about $8.75\,\text{dB}$. The DGS sensor enhanced the detection of the buried target by $\sim 10\,\text{dB}$.

In the Second case, the soil is described as "Red clay soil", with an electrical properties of $\varepsilon_r = 8.1$, $\mu_r = 1.0$, and $\sigma = 0.038\,\text{s/m}$. all the different targets in the first case of study will also be detect

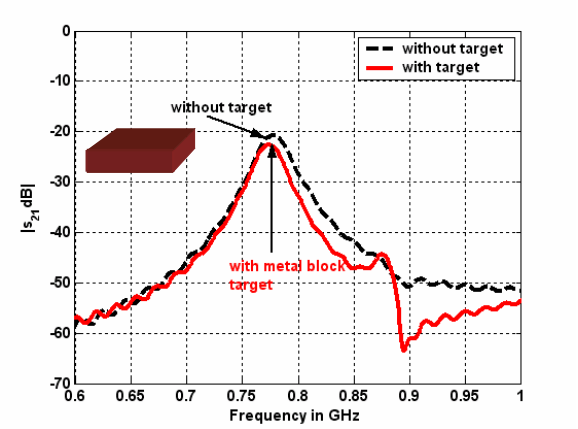

Figure 8. $|S_{21}|$ of classic sensor to detect metal block target buried in soil with $\varepsilon_r = 2.9$ using FDTD simulation at $f_o = 790\,\text{MHz}$.

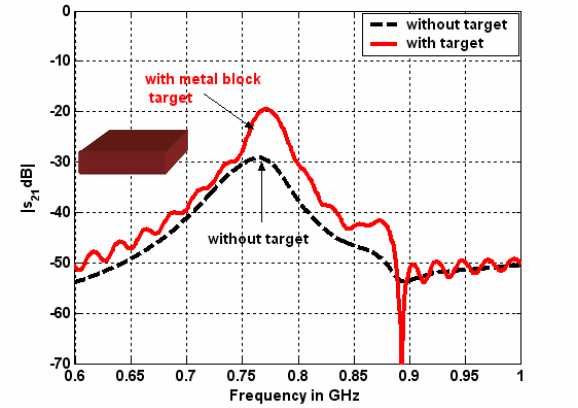

Figure 9. $|S_{21}|$ of DGS Sensor to detect metal block target buried in soil with $\varepsilon_r = 2.9$ using FDTD simulation at $f_o = 790\,\text{MHz}$.

in the second case of study. In case of detecting the circular bakelite target with electrical properties mentioned above. Fig. 10 shows the calculated mutual coupling, $|S_{21}|$, resulting from using the classical sensor in case of absence and presence of the target is $-21.38\,\text{dB}$ and $-16.1\,\text{dB}$, respectively. The classical sensor enhanced the detection of the buried target by $\sim 5\,\text{dB}$.

If the DGS sensor is simulated to detect the same *bakelite target* with the same electrical properties in the same soil properties. Fig. 11 shows the calculated mutual coupling, $|S_{21}|$, resulting from using the

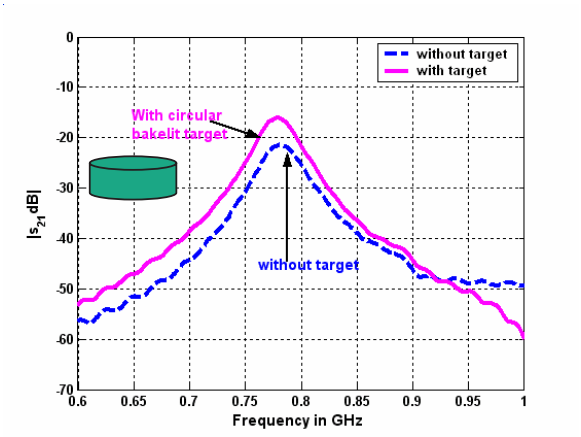

Figure 10. $|S_{21}|$ of classic sensor to detect circular Bakelite target buried in soil with $\varepsilon_r = 8.1$ using FDTD simulation at $f_o = 790\,\text{MHz}$.

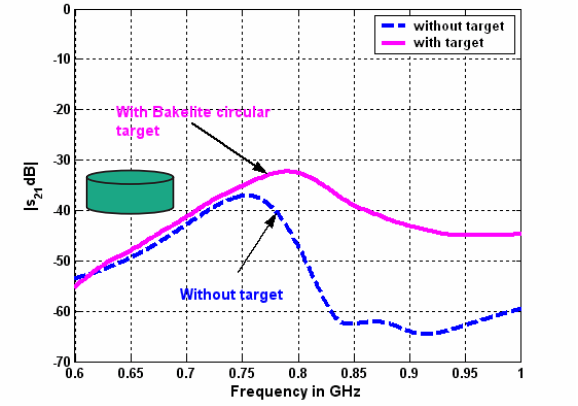

Figure 11. $|S_{21}|$ of DGS Sensor detect circular Bakelite target buried in soil with $\varepsilon_r = 8.1$ using FDTD simulation at $f_o = 790\text{MHz}$.

DGS sensor in case of absence and presence of the target are $-37.2\,\text{dB}$ and $-31.7\,\text{dB}$, respectively. The DGS sensor enhanced the detection of the buried target by $\sim 6\,\text{dB}$.

If the buried target in the same soil *is metal block target* contains TNT material. The target characteristics are block shape with length $= 241.15\,\text{mm}$, width $= 86.57\,\text{mm}$, depth $= 55.94\,\text{mm}$, weight $= 100\,\text{g}$, and $\sigma = 58 \times 10^{12}\,\text{s/m}$. The TNT material with electrical properties of $\varepsilon_r = 3.0$, $\mu = 1.0$, and $\sigma = 0.0029\,\text{s/m}$. Fig. 12 shows the calculated mutual coupling, $|S_{21}|$, resulting from using the classical

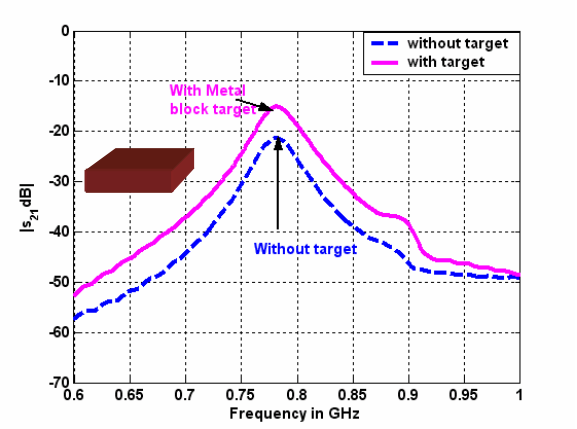

Figure 12. $|S_{21}|$ of classic sensor to detect block metal target buried in soil with $\varepsilon_r = 8.1$ using FDTD simulation at $f_o = 790\,\text{MHz}$.

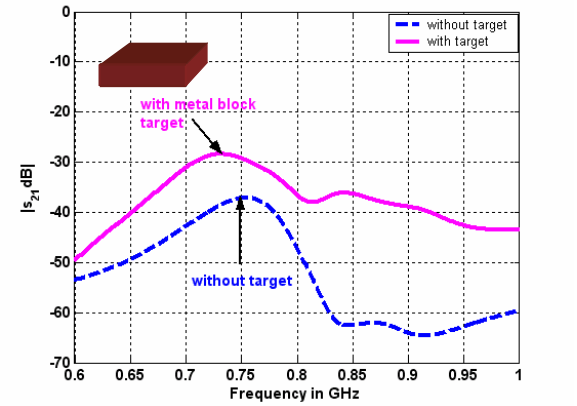

Figure 13. $|S_{21}|$ of DGS Sensor to detect metal block target buried in soil with $\varepsilon_r = 8.1$ using FDTD simulation at $f_o = 790\,\text{MHz}$.

sensor in case of the absence the presence of the target is $-20.78\,\text{dB}$ and $-15\,\text{dB}$, respectively. The classical sensor enhanced the detection of the buried target by $\sim 6.5\,\text{dB}$.

If the DGS sensor is simulated to detect the above *metal block target* with same electrical properties and in the same soil properties. Fig. 13 shows the calculated mutual coupling, $|S_{21}|$, resulting from using the DGS sensor in case of the absence and presence of the target is $-37.2\,\text{dB}$ and $-28.6\,\text{dB}$, respectively. The DGS sensor enhanced the detection of the buried target by $\sim 9\,\text{dB}$.

3. CONCLUSION

The FDTD simulation has been used to simulate the detection process of the buried targets using a new proposed sensor. It consists of two parallel microstrip antennas that are placed on same ground plane with defected ground structure between them. The proposed sensor has the advantage of low mutual coupling between the elements of the array and more detecting capability compared with the classical sensor. The detecting capability depends on the types of the soil and targets.

REFERENCES

1. Boutros-Ghali, B., "The land mine crisis," *Foreign Affairs*, Vol. 73, 8–13, Sept.–Oct. 1994.
2. Paik, J. K., C. P. Lee, and M. A. Abidi, "Image processing-based mine detection techniques using multiple sensors: A review," *Subsurface Sensing Technologies and Applications: An International Journal*, Vol. 3, No. 3, 153–202, July 2002.
3. Van den Bosch, I., S. Lambot, M. Acheroy, I. Huynen, and P. Druyts, "Accurate and efficient modeling of monostatic GPR signal of dielectric targets buried in stratified media," *Journal of Electromagnetic Waves and Applications*, Vol. 20, No. 3, 283–290, 2006.
4. Chen, X., D. Liang, and K. Huang, "Microwave imaging 3-D buried objects using parallel genetic algorithm combined with FDTD technique," *Journal of Electromagnetic Waves and Applications*, Vol. 20, No. 13, 1761–1774, 2006.
5. Xue, W. and X.-W. Sun, "Target detection of vehicle volume detection radar based on Winger-Hough transform," *Journal of Electromagnetic Waves and Applications*, Vol. 21, No. 11, 1513–1523, 2007.
6. Bourgeois, J. M. and G. S. Smith, "A complete electromagnetic simulation of the separated-aperture sensor for detecting buried land mines," *IEEE Trans. Antennas Propagat.*, Vol. 46, 1419–1426, Oct. 1998.
7. Zainud-Deen, S. H., M. E. Badr, K. H. Awadalla, and H. A. Sharshar, "Microstrip antenna for detecting buried land mines," *23rd NRSC2006 Symp.*, Faculty of Electronic Engineering, Menoufya, Univ. Egypt, March 14–16, 2006.
8. Zainud-Deen, S. H., M. E. Badr, K. H. Awadalla, and H. A. Sharshar, "Microstrip antenna with shorting pins as a sensor for landmines detecting," *24th NRSC2007 Symp.*, Faculty

of Engineering, Ain Shams, Univ. Cairo, Egypt, March 13–15, 2007.

9. Zainud-Deen, S. H., M. E. Badr, E. El-Deen, K. H. Awadalla, and H. A. Sharshar, "MIcrostrip antenna with corrugated ground plane surface as a sensor for landmines detection," *Process In Electromagnetics Research B*, Vol. 2, 259–278, 2008.
10. Nikolic, M. M., R. A. Djordevic, and A. Nehorai, "Microstrip antennas with suppressed radiation in horizontal directions and reduced coupling," *IEEE Trans. Antennas Propagat.*, Vol. 53, No. 11, 3469–3476, Nov. 2005.
11. Salehi, M. and A. Tavakoli, "A novel mutual coupling microstrip antenna array designs using defected ground structure," *Int. J. Electron Commun. (AEU)*, Vol. 60, 718–723, 2006.
12. Yee, K. S., "Numerical solution of initial boundary value problems involving Maxwell's equations in isotropic media," *IEEE Trans. Antennas Propagat.*, Vol. 14, 302–307, 1966.
13. Taflove, A., *Computational Electrodynamics: The Finite Difference Time Domain Method*, Artech House, Norwood, MA, 2000.